

Accurate extraction of thermal expansion coefficients and their uncertainties from high precision interferometric length measurements

R. Schödel*

Physikalisch-Technische Bundesanstalt (PTB), Braunschweig, Germany

The evaluation of the coefficient of thermal expansion (CTE) from the observed temperature induced length changes becomes the more difficult the lower the final uncertainty of the CTE is desired. On a scale of nanometers the length as a function of the sample temperature clearly deviates from the linear approximation so that higher polynomials are used as fit functions to the measured data. From such polynomials of a certain degree the CTE can easily be evaluated according to its definition. In this paper it is demonstrated in which way the corresponding uncertainty of the CTE can be calculated in accordance with the GUM what is done on the basis of symbolic computation by means of *MATHEMATICA*[®]. On the other hand, the arbitrariness of the choice of the polynomial order causes an additional uncertainty contribution as discussed in this paper. Examples are given to illustrate the mentioned problems.

Keywords: thermal expansion, expansivity, interferometer, absolute length measurements

1. INTRODUCTION

Phase shifting interferometry, in combination with computer-based analysis of interference phase maps, has almost replaced traditional methods in interferometric length measurements and special attention was paid in order to reduce the measurement uncertainty [1, 2, 3]. In the case of thermal expansion measurements by interferometric length measurements the uncertainty of the length changes determined from the differences of the measured lengths could be reduced to the range of sub-nanometers [e.g. see 4]. However, the accurate extraction of the coefficient of thermal expansion (CTE) from such precise data requires a careful and critical analysis as outlined in this paper.

There exist alternative definitions of the CTE as examined in [5]. The “true” CTE (also referred as thermal expansivity) is defined according to the following equation:

$$\alpha = \frac{1}{L} \cdot \frac{dL}{dT} \quad (1)$$

This definition bases on the knowledge of the derivative term dL/dT as a function of the temperature. Often the temperature dependence of the length, L , in the denominator is ignored because of its small influence so that α is calculated from:

$$\alpha \approx \frac{1}{L_0} \cdot \frac{dL}{dT} \quad (2)$$

As an example, for a 100 mm steel gauge block ($\alpha \approx 10^{-5} \text{ K}^{-1}$), where L_0 is assigned to the length at 20°C the difference between eq. 1 and eq. 2, $\alpha \cdot (L_0 - L)/L_0$, amounts to $\approx 10^{-9} \text{ K}^{-1}$ at the temperatures of 10°C or 30°C. If such differences are in the order of the uncertainty desired, it becomes essential to define the CTE according to eq. 1.

* rene.schoedel@ptb.de; phone: +49 531 592 5420; fax: +49 531 592 69 5420; Physikalisch-Technische Bundesanstalt (PTB), Bundesallee 100, D-38116 Braunschweig

Recent Developments in Traceable Dimensional Measurements III, edited by Jennifer E. Decker, Gwo-Sheng Peng, Proceedings of SPIE Vol. 5879 (SPIE, Bellingham, WA, 2005) · 0277-786X/05/\$15 · doi: 10.1117/12.616923

Considering a measured data set of $\{t_i, l_i\}$ (data points of temperature and length), an average CTE, α^{av} , can be defined in the temperature interval $\{t_i, t_{i+1}\}$ of neighbouring data points according to the difference quotient:

$$\alpha^{av}(\bar{t}_i) = \frac{1}{\bar{l}_i} \cdot \frac{\Delta l_i}{\Delta t_i}, \quad (3)$$

where $\bar{t}_i = \frac{1}{2}(t_i + t_{i+1})$, $\bar{l}_i = \frac{1}{2}(l_i + l_{i+1})$ and $\Delta l_i = l_{i+1} - l_i$ is the length difference corresponding to the temperature difference $\Delta t_i = t_{i+1} - t_i$. The limiting case $\Delta t_i \rightarrow 0$ leads to the definition of the CTE according to eq. 1. However, the uncertainty of the differential quotient increases dramatically. Therefore, another strategy is useful to obtain the derivative term dL/dT . It consists of a least square fitting procedure with respect to the data set $\{t_i, l_i\}$ resulting in a polynomial of the degree n which describes the length of a sample (e.g. gauge block) as a function of the temperature T :

$$L^{(n)} = a_0 + a_1(T - T_0) + a_2(T - T_0)^2 + \dots + a_n(T - T_0)^n, \quad (4)$$

where T_0 is an arbitrary reference temperature, e.g. 20°C. Such polynomial can simply be used for the evaluation of the CTE according to:

$$\alpha^{(n)} = \frac{1}{L^{(n)}} \cdot \frac{dL^{(n)}}{dT} = \frac{a_1 + a_2(T - T_0) + \dots + a_n(T - T_0)^{n-1}}{a_0 + a_1(T - T_0) + a_2(T - T_0)^2 + \dots + a_n(T - T_0)^n} \quad (5)$$

$n = 1$ in eq.5 corresponds to a quasi constant CTE. However, n is larger than 1 as measurements reveal in general (e.g. see below). As it is obvious from eq. 5 the "true" CTE is not of the simple form $\alpha_0 + \alpha_1(T - T_0) + \dots$. Only the approximate definition according to eq. 2 leads to this form.

2. RESULTS AND DISCUSSION

2.1 Calculation of CTE's uncertainty

As outlined above the thermal expansion coefficient is calculated on the basis of a polynomial $L^{(n)} = a_0 + a_1\vartheta + a_2\vartheta^2 + \dots + a_n\vartheta^n$, where a_0 corresponds to the gauge block length at a certain temperature T_0 (e.g. 20°C) and $\vartheta = (T - T_0)$. Polynomials of a certain degree n can be obtained by least square fitting. Such fitting can easily be done numerically resulting in numerical expressions for the coefficients a_i . However, it is impossible to calculate their uncertainties in accordance with the GUM, where sensitivity coefficients of the form $\partial a_k / \partial \vartheta_i$ are involved.

An effective way of uncertainty evaluation is the use of symbolic computation by *MATHEMATICA*[®] (Wolfram Research, v. 5). The basic principle of the "symbolic" fitting is the same as for the numerical fitting: the minimization of the χ^2 . The difference consists in the fact that the measured data are replaced by symbols. Just in a final step the data are inserted into the symbolic expressions. This gives the possibility to calculate derivatives of the resulting coefficients in order to extract sensitivities as required by the GUM. In addition, in the calculation of χ^2 weighted addends can be used according to:

$$\chi^2 = \sum_{i=1}^N p_i \cdot (l_i - L^{(n)}(\vartheta_i))^2, \quad (6)$$

where N is the number of data points. The weights, p_i , are numerical expressions assigned according to the uncertainties of the individual length and temperature measurements:

$$p_i = \frac{1}{u(l_i)^2 + (l_i \cdot \alpha_{re} \cdot u(\vartheta_i))^2}, \quad (7)$$

where α_{re} is a rough estimate of the CTE, $u(l_i)$ is the uncertainty of the measured length and $u(\vartheta_i)$ that of the temperature.

The minimum of the χ^2 is obtained from the (symbolic) solution of the set of $n + 1$ equations:

$$\frac{\partial}{\partial a_k}(\chi^2) = 0 \quad k = 0 \dots n, \quad (8)$$

resulting in symbolic expressions for the coefficients a_k of the polynomial fit. Dependent on the polynomial degree, the expressions a_k can be very voluminous. However, even very large expressions can be simply used for further computation in *MATHEMATICA*[®] and there is no need for a simplification. The uncertainties of the a_k are calculated according to:

$$u(a_k) = \sqrt{\sum_{i=1}^N \left\{ \left(\frac{\partial a_k}{\partial l_i} \cdot u(l_i) \right)^2 + \left(\frac{\partial a_k}{\partial \vartheta_i} \cdot u(\vartheta_i) \right)^2 \right\}}, \quad (9)$$

what is in accordance with the GUM. An alternative way for the calculation of $u(a_k)$ is to transform the uncertainty of the temperature into an additional length uncertainty as already done in the definition of the weights (eq. 7). This approach leads to:

$$u(a_k) = \sqrt{\sum_{i=1}^N \left\{ \left(\frac{\partial a_k}{\partial l_i} \right)^2 \cdot \left([u(l_i)]^2 + (l_i \cdot \alpha_{re} \cdot u(\vartheta_i))^2 \right) \right\}}, \quad (9a)$$

Using eq. 5 the CTE is obtained from the differentiation $L^{(n)}$ divided by $L^{(n)}$. Again in accordance with the rules of the GUM, the uncertainty of the CTE can be obtained from:

$$u(\alpha) = \sqrt{\sum_{k=0}^n \left\{ \left(\frac{\partial \alpha}{\partial a_k} \cdot u(a_k) \right)^2 \right\}} \quad (10)$$

In a final step the measured data $\{\vartheta_i, l_i\}$ and their estimated uncertainties $\{u(\vartheta_i), u(l_i)\}$ can be inserted so that numeric expressions for a_k and $u(a_k)$ and therewith numeric functions of α and $u(\alpha)$ are returned.

2.2 Additional uncertainty contribution due to the arbitrariness of the fit polynomial

The straight forward calculation of $u(\alpha)$ resulting in eq. 10 presumes that the temperature induced length changes can be described by a certain polynomial of the degree n . However, the functional relationship between the length and the temperature for a given material is not known on the nm-scale. Therefore, the choice of the polynomial degree in eq. 4 is arbitrary. There is an unknown deviation of the material inherent CTE compared to the CTE obtained from eq. 5 which can by far exceed $u(\alpha)$ obtained from eq. 10. This problem is demonstrated by an example which basis on simulated values of sample lengths at given temperatures. The following assumptions are made for the simulation: a sample of $L_0 = a = 0.197840$ m at $T_0 = 20^\circ\text{C}$ has a temperature dependent length which is given by a polynomial of the degree 2:

$$L^{sim} = a + b \vartheta + c \vartheta^2, \quad \vartheta = T - T_0, \quad (11)$$

where $b/a = 2.5554 \cdot 10^{-6} \text{ K}^{-1}$, $c/a = 4.58 \cdot 10^{-9} \text{ K}^{-2}$ (these quantities base on [6] found for single crystal silicon). The corresponding CTE is obtained from eq. 1:

$$\alpha^{sim} = \frac{b + 2c \vartheta}{a \cdot (1 + b/a \vartheta + c/a \vartheta^2)} \quad (12)$$

and is approximately given by: $\alpha^{sim} \cong b/a + 2c/a \vartheta$ (eq. 2). A simulated data set $\{\vartheta_i^{sim}, l_i^{sim}\}$ is generated on the basis of eq. 11 according to the following definition:

$$\begin{aligned} \vartheta_i^{sim} &= \text{Random} \left[\text{NormalDistribution} \left[\vartheta_i, u(\vartheta_i) \right] \right] \\ l_i^{sim} &= \text{Random} \left[\text{NormalDistribution} \left[a + b \vartheta_i + c \vartheta_i^2, u(l_i) \right] \right] \end{aligned} \quad (13)$$

where ϑ_i denotes the deviation from 20°C for selected temperatures in the temperature range between 15°C and 25°C . The phrase $\text{Random}[\text{NormalDistribution}[x, u(x)]]$ means that normal distributed random values are generated, where x denotes the mean value and $u(x)$ its standard deviation. A number of 11 temperatures seems appropriate (or even large) compared with the typical number of data points in a series of interferometric length measurements.

For simplicity the uncertainties $\{u(\vartheta_i), u(l_i)\}$ are set to be identical at each data point in the simulations. Two different sets of values $\{u(\vartheta), u(l)\}$ are considered in the example:

$$\begin{aligned} \text{Set A:} & \quad u(\vartheta) = 10 \text{ mK}, & u(l) = 10 \text{ nm} \\ \text{Set B:} & \quad u(\vartheta) = 1 \text{ mK}, & u(l) = 1 \text{ nm.} \end{aligned}$$

The data related to these sets are labeled by A and B, respectively, in the following figures. Fig. 1 shows the simulated data (data points) together with solid lines representing the linear case (polynomials with $n = 1$) which virtually seem to fit to the data in A and B on a scale of μm .

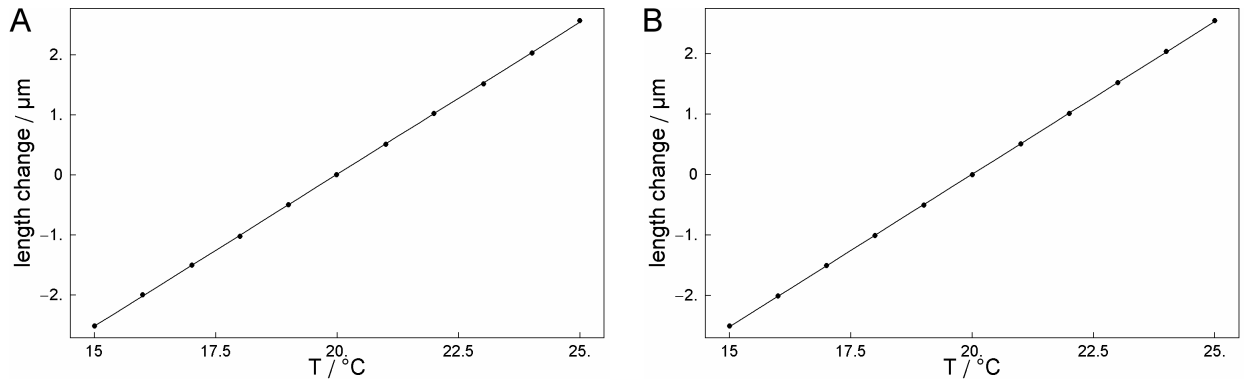


Figure 1 Simulated data (data points) of the length change as a function of the temperature for case A (left, uncertainties: {10 mK, 10 nm}) and for case B (right, uncertainties: {10 mK, 10 nm}). The straight lines represent linear fit polynomials.

The deviations of the data points from the linear fits of Fig. 1 are shown on the top of Fig. 2A and B, respectively. In case B the systematic deviations (which exist by definition using eq.11) become visible because of the low uncertainties ({1 mK, 1 nm}) what is not the case for A ({10 mK, 10 nm}). The other graphs show the deviation of the higher order fit polynomials ($n = 2, n = 3$) from the simulated data. The variance of the data specified in the graphs is calculated according to:

$$\text{VARIANCE} = \sqrt{\frac{\sum_{i=1}^N (l_i - L^{(n)}(v_i))^2}{N - (n + 1)}}, \quad (14)$$

which is similar to the RMS but takes into account for the number of free parameters which is $n + 1$ for a polynomial of the degree n . This is important because of the relatively small number of data points, N , keeping in mind that a polynomial of the degree $n = N - 1$ perfectly “fits” the data because it is the interpolating polynomial.

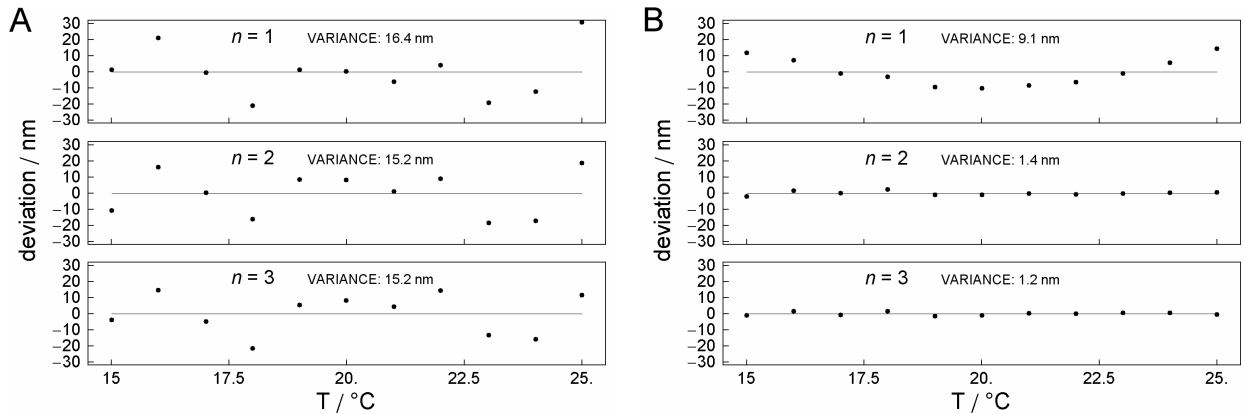


Figure 2 Deviations of the data points of Fig. 1 from the fit polynomial of the degree n for case A (left, uncertainties: {1 mK, 1 nm}) and for case B (right, uncertainties: {1 mK, 1 nm})

In the case of Fig. 2A ({10 mK, 10 nm}) the variance is almost unaffected by the choice of the polynomial degree and is similar compared with:

$$\tilde{u}(l) = \sqrt{(u(l))^2 + (l \cdot \alpha_{re} \cdot u(\vartheta))^2}, \quad (15)$$

which results in 11.2 nm for the case A. Thus, in case A it is impossible to extract systematic information about the characteristics of the length as a function of the temperature. This is different in Fig. 2B where the variance is drastically reduced (from 9.1 nm to 1.4 nm) when $n=2$ is used instead of $n=1$ so that the case $n=1$ can be discriminated. It should be pointed out again that the case $n=2$ represents the functional relationship as set for the simulation (eq. 11). For $n=3$ a slightly reduced variance is found in case B, whereas for both, $n=2$ and $n=3$, the variance is comparable with the value of 1.1 nm which results from eq. 15 for B ($\{1 \text{ mK}, 1 \text{ nm}\}$). Thus, $n=3$ cannot be discriminated in case B (as, of course, in case A).

In Fig. 3 for each case, A and B, the CTEs resulting from the linear fit polynomial ($n=1$) according to eq. 5 is shown as solid line. The corresponding uncertainties obtained from eq. 9 are shown as dark grey regions around the solid lines in A and B. The dashed lines represent the actual CTE as defined in this simulation by eq. 12. For comparison the average CTE values obtained from the difference quotient of neighbouring data (eq. 3) are shown as points in Fig. 3.

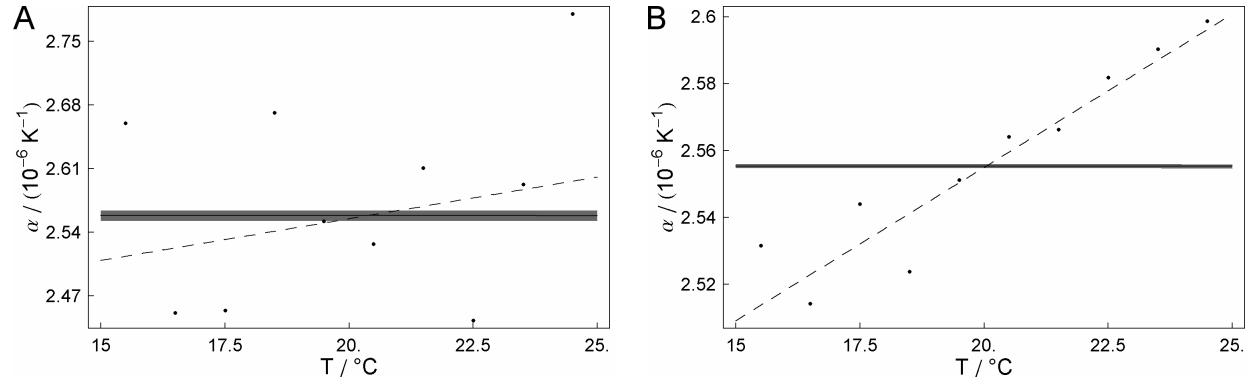


Figure 3 CTEs resulting from the linear fit polynomial ($n=1$) according to eq. 5 (solid lines) and uncertainties obtained from eq. 9 (dark grey regions around the solid lines) for case A and B. Dashed lines represent the actual CTE as defined by eq. 12. Data points indicate the average CTEs according to eq. 3.

As can be seen in Fig. 3 A and B the evaluated uncertainties (dark grey regions) overlap with the actual CTE (dashed lines) only at the temperature $T_0 = 20^\circ\text{C}$. At other temperatures the deviation between the (constant) CTE and the actual CTE becomes large. This is important for case A where it is impossible to discriminate the value of $n=1$ in the fit polynomial. Thus, in such case the amount of uncertainty evaluated from the linear fit polynomial is dramatically underestimated.

Fig. 4 shows the CTE for the case A and B resulting from the fit polynomials using $n=2$ according to eq. 5 (solid lines). The resultant uncertainties obtained from eq. 10 are shown as grey regions. $n=2$ represents the functional relationship between the length and the temperature as assumed in the simulation via eq. 11. Therefore, it is remarkable that the actual CTE as defined in the simulation by eq. 12 (dashed lines) is covered by the uncertainties in both cases. This result was checked for various different random data sets according to eq. 13 (data not shown) and confirms that the uncertainties are calculated properly.

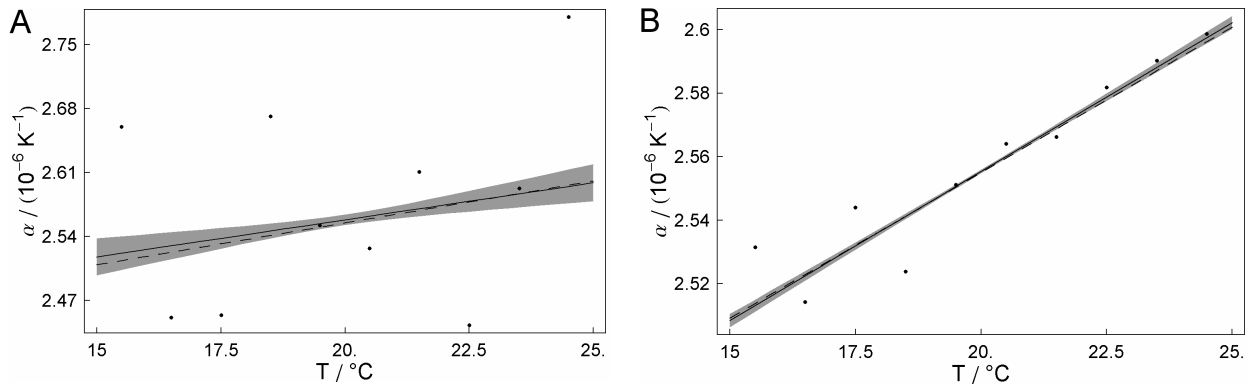


Figure 4 CTEs resulting from the fit polynomial using $n = 2$ according to eq. 5 (solid lines) and uncertainties obtained from eq. 9 (grey regions around the solid lines) for case A and B. Dashed lines represents the actual CTE as defined by eq. 12. Data points indicate the average CTEs according to eq. 3.

As already mentioned, the results shown in Fig. 4 are in good agreement with the assumed model, i.e. α^{sim} by eq. 12. However, this information, i.e. the degree of the polynomial, is not available in the case of actual measurements. Therefore, it is useful (especially in case B) to investigate $n = 3$. Fig. 5 shows the resulting CTE for case A and B as solid lines surrounded by light grey regions representing the corresponding uncertainties. The latter are clearly larger than in the case $n = 2$ (see Fig. 4). It is a general rule that the larger n the larger are the resulting uncertainties (via eq. 10). This can easily be explained by the increased number of parameters ($n + 1$) in the model and does not contradict to the fact, that the variance of the data as in Fig. 2 is typically reduced.

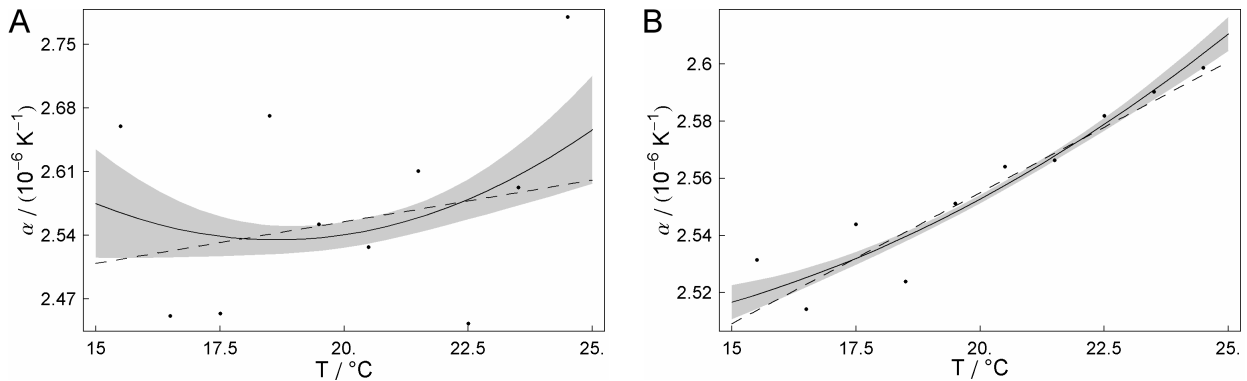


Figure 5 CTEs resulting from the fit polynomial using $n = 3$ according to eq. 5 (solid lines) and uncertainties obtained from eq. 9 (light grey regions around the solid lines) for case A and B. Dashed lines represents the actual CTE as defined by eq. 12. Data points indicate the average CTEs according to eq. 3.

Fig. 6 summarizes the results shown in Figs. 3 - 5 and Tab. 1 lists the data for the three temperatures 15°C, 20°C and 25°C.

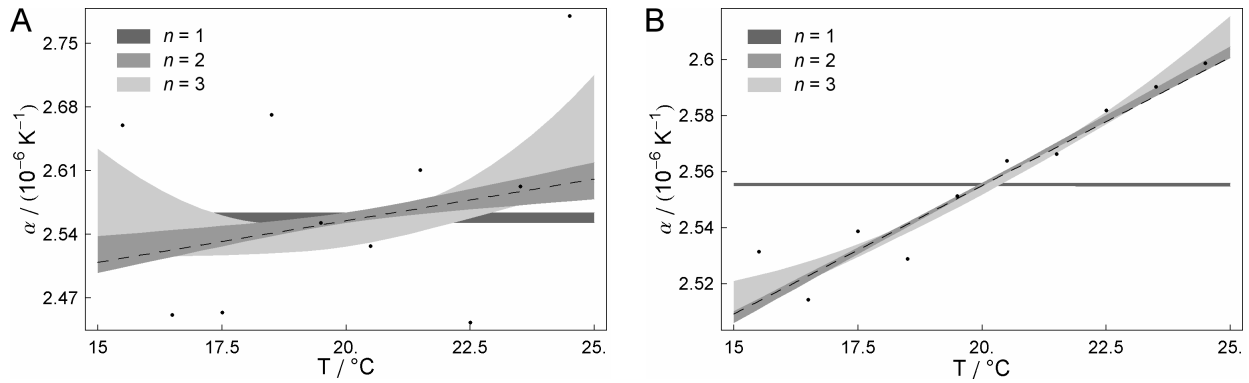


Figure 6 Summary of the data shown in Figs. 3 - 5.

A					B				
T / °C	α^{sim}	$\alpha^{(1)}$	$\alpha^{(2)}$	$\alpha^{(3)}$	T / °C	α^{sim}	$\alpha^{(1)}$	$\alpha^{(2)}$	$\alpha^{(3)}$
		$u(\alpha^{(1)})$	$u(\alpha^{(2)})$	$u(\alpha^{(3)})$			$u(\alpha^{(1)})$	$u(\alpha^{(2)})$	$u(\alpha^{(3)})$
15	2.5096	2.5584	2.5178	2.5749	15	2.5096	2.5554	2.5082	2.5151
		0.0054	0.0201	0.0592			0.0005	0.0020	0.0059
20	2.5554	2.5584	2.5584	2.5406	20	2.5554	2.5554	2.5554	2.5533
		0.0054	0.0054	0.0139			0.0005	0.0005	0.0014
25	2.6012	2.5584	2.5990	2.6562	25	2.6012	2.5554	2.6027	2.6096
		0.0054	0.0201	0.0592			0.0005	0.0020	0.0059

Table 1 Listing of the CTEs resulting from the fit polynomial using $n = 1, 2$ and 3 according to eq. 5 and uncertainties obtained from eq. 10 for case A and B for the temperatures 15°C , 20°C and 25°C . α^{sim} denotes the actual CTE as defined in the simulations by eq. 12.

Fig. 6 separately lists the uncertainties of the CTEs according to eq. 10 for $n = 1, 2$ and 3 in case A and B. In addition the differences between CTEs obtained from the polynomials of different degree are shown (solid lines).

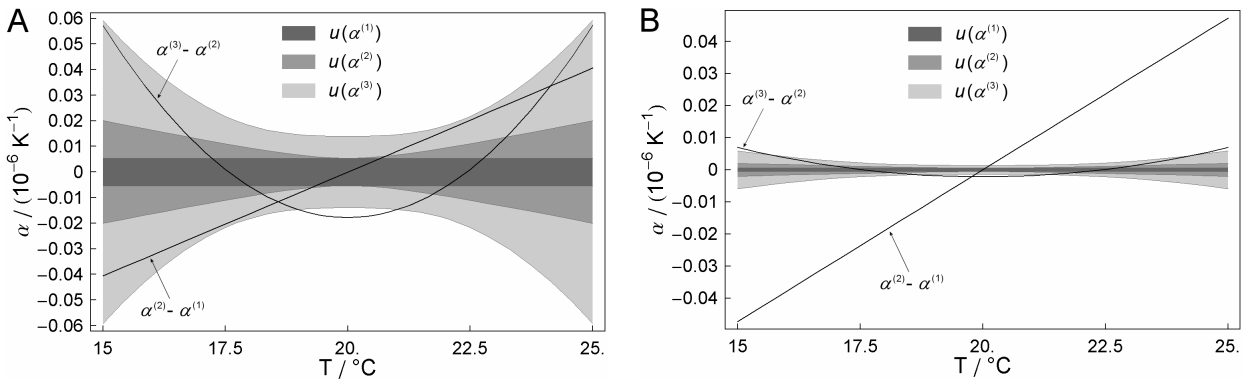


Figure 7 CTE-uncertainties according to eq. 10 for $n = 1, 2$ and 3 in case A and B together with the differences between CTEs obtained from the polynomials of different degree.

In case A it is obvious that the deviation $\alpha^{(2)} - \alpha^{(1)}$ is up to almost one order of magnitude larger than the estimated uncertainty obtained from eq. 10 for $n = 1$. Therefore, since $\alpha^{(2)}$ in principle represents α^{sim} (see Tab. 1), the actual uncertainty of the CTE is dramatically underestimated when it is identified with $u(\alpha^{(1)})$. This situation is even worse in case B, however, $n = 1$ could be ruled out in this case (see Fig. 2). Continuing with case A, Fig. 7 shows that also the difference $\alpha^{(3)} - \alpha^{(2)}$ is clearly larger than $u(\alpha^{(2)})$. Thus, $u(\alpha^{(2)})$ obtained from eq. 10 for $n = 2$ can also not be identified with a reliable uncertainty in case A. This situation is again the same in case B.

As an attempt for the estimation of a total uncertainty the deviation $\alpha^{(n+1)} - \alpha^{(n)}$ is taken as a additional uncertainty contribution according to:

$$u_{total}(\alpha^{(n)}) = \sqrt{\left(u(\alpha^{(n)})\right)^2 + \left(\alpha^{(n+1)} - \alpha^{(n)}\right)^2} \quad (16)$$

Fig. 8 A shows $\alpha^{(1)}$ according to eq. 5 (solid lines) together with its uncertainty u_{total} according to eq. 16. It is noticeable in case A that $\alpha^{(1)} \pm u_{total}$ does not quite cover α^{sim} (indicated by the dashed line). However, this situation does not contradict to any assumption since u_{total} is a standard uncertainty (about 68% probability). For other random data sets (not shown) $\alpha^{(1)} \pm u_{total}$ typically covers α^{sim} . Although the case $n = 1$ can be excluded in case B, for the sake of completeness Fig. 8 B shows $\alpha^{(1)} \pm u_{total}$ for that case.

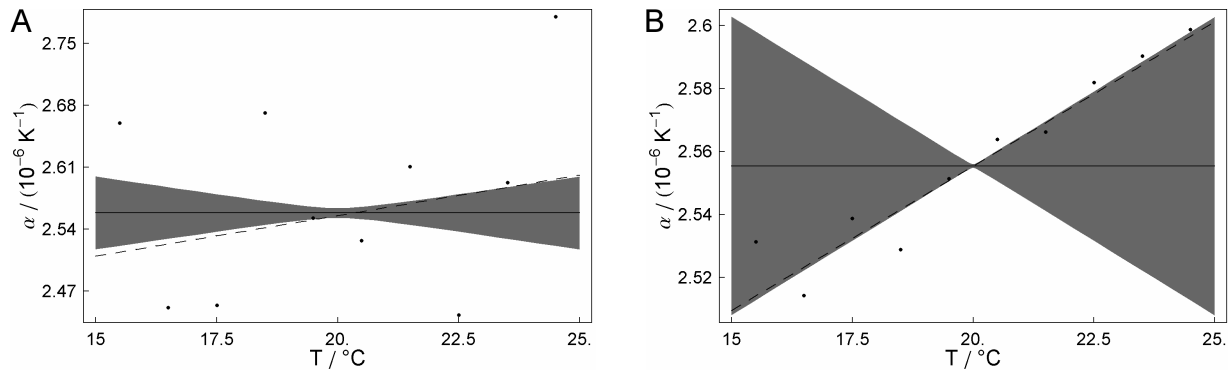


Figure 8 CTEs for $n = 1$, i.e. $\alpha^{(1)}$ (solid lines) together with their total uncertainties according to eq. 16 for the case A and B. Dashed lines represents the actual CTE as defined by eq. 12. Data points indicate the average CTEs according to eq. 3.

Fig. 9 shows $\alpha^{(2)}$ according to eq. 5 (solid lines) together with the uncertainties u_{total} for $n = 2$ according to eq. 16 for the case A and B. In both cases $\alpha^{(2)} \pm u_{total}$ cover the data of α^{sim} (indicated by the dashed line). Tab. 2 shows the values of $\alpha^{(1)}$, $\alpha^{(2)}$ and u_{total} from Fig. 8 and Fig. 9 at the temperatures 15 $^{\circ}\text{C}$, 20 $^{\circ}\text{C}$ and 25 $^{\circ}\text{C}$ for the two cases A and B, respectively.

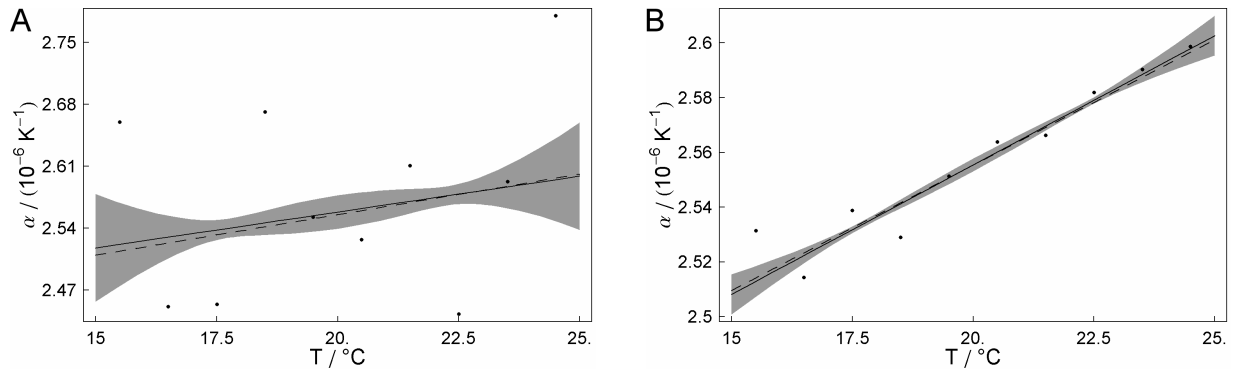


Figure 9 CTEs for $n = 2$, i.e. $\alpha^{(2)}$ (solid lines) together with their total uncertainties according to eq. 16 for the case A and B. Dashed lines represents the actual CTE as defined by eq. 12. Data points indicate the average CTEs according to eq. 3.

T / °C	α^{sim}	units: $10^{-6} K^{-1}$	
		$\alpha^{(1)}$ $u(\alpha^{(1)})$	$\alpha^{(2)}$ $u(\alpha^{(2)})$
15	2.5096	2.5584	2.5178
		0.0410	0.0606
20	2.5554	2.5584	2.5584
		0.0054	0.0186
25	2.6012	2.5584	2.5990
		0.0410	0.0606

T / °C	α^{sim}	units: $10^{-6} K^{-1}$	
		$\alpha^{(1)}$ $u(\alpha^{(1)})$	$\alpha^{(2)}$ $u(\alpha^{(2)})$
15	2.5096	2.5554	2.5082
		0.0473	0.0072
20	2.5554	2.5554	2.5554
		0.0005	0.0022
25	2.6012	2.5554	2.6027
		0.0473	0.0072

Table 2 Listing of the CTEs resulting from the fit polynomial using $n = 1, 2$ and 3 according to eq. 5 and uncertainties obtained from eq. 9 for case A and B for the temperatures $15^\circ C, 20^\circ C$ and $25^\circ C$. α^{sim} denotes the actual CTE as defined by eq. 12.

3. CONCLUSIONS

The accurate extraction of the coefficient of thermal expansion (CTE) from measurements of the absolute length as a function of the temperature by interferometry requires a careful and critical analysis. A so called “true” CTE (also referred as thermal expansivity) can be evaluated assuming a polynomial fit to the data. There exists a very effective way of uncertainty evaluation in accordance with the GUM using symbolic computation. However, the degree n of the polynomial, i.e. the type of the functional relationship between the length and the temperature for a given material, is not known on the nm-scale. Therefore, the choice of the polynomial degree n is arbitrary and there is an unknown deviation of the material inherent CTE compared to the CTE obtained from the polynomial fit. Such deviation is demonstrated by means of a simulated data set generated on the basis of an example polynomial ($n = 2$) for two different cases of uncertainties. In the case of lower uncertainties ($\{1 \text{ mK}, 1 \text{ nm}\}$) the systematic deviations of the data points from the linear fits is clearly visible so that $n = 1$ can be discriminated. This is different in the case of the larger uncertainties ($\{10 \text{ mK}, 10 \text{ nm}\}$) where the variance of the deviation of the data from the fit is almost unaffected by the choice of the assumed polynomial order. In such case it is impossible to extract systematic information about the characteristics of the length as a function of the temperature so that the amount of uncertainty evaluated considering a linear fit polynomial is dramatically underestimated. As a suggestion for the estimation of a total uncertainty, the deviation $\alpha^{(n+1)} - \alpha^{(n)}$ can be taken into account as an additional uncertainty contribution.

REFERENCES

1. G. Bönsch 2001. Automatic gauge block measurements by phase stepping interferometry with three laser wavelengths. Proc. SPIE 4410:1-10 (2001).
2. R. Schödel, G. Bönsch, Highest accuracy interferometer alignment by retroreflection scanning, Applied Optics 43, 5738-5743 (2004).
3. J. E. Decker, R. Schödel and G. Bönsch. Considerations for the evaluation of measurement uncertainty in interferometric gauge block calibration applying methods of phase step interferometry. Metrologia 41:L11-L17 (2004).
4. R. Schödel, A. Nicolaus and G. Bönsch. Minimizing interferometer misalignment errors for measurement of sub-nanometer length changes. In Recent Developments in Traceable Dimensional Measurements II, Decker, Brown, eds., Proc. SPIE 5190:34-42 (2003).
5. J.D. James, J. A. Spittle, S.G.R. Brown and R.W. Evans. A review of measurement techniques for the thermal expansion coefficient of metals and alloys at elevated temperatures. Meas. Sci. Technol. 12, R1–R15 (2001)
6. R. Schödel and G. Bönsch. Precise interferometric measurements at single crystal silicon yielding thermal expansion coefficients from 12 °C to 28 °C and compressibility. Proc. SPIE 4410:54-62 (2001).